Unsteady Electroosmotic Channel Flows with the Nonoverlapped and Overlapped Electric Double Layers

Sangmo Kang*, Yong Kweon Suh
Department of Mechanical Engineering, Dong-A University, Busan 604-714, Korea

In micro- and nanoflows, the Boltzmann distribution is valid only when the electric double layers (EDL's) are not overlapped and the ionic distributions establish an equilibrium state. The present study has numerically investigated unsteady two-dimensional fully-developed electroosmotic flows between two parallel flat plates in the nonoverlapped and overlapped EDL cases, without any assumption of the Boltzmann distribution. For the study, two kinds of unsteady flows are considered : one is the impulsive application of a constant electric field and the other is the application of a sinusoidally oscillating electric field. For the numerical simulations, the ionic-species and electric-field equations as well as the continuity and momentum ones are solved. Numerical simulations are successful in accurately predicting unsteady electroosmotic flows and ionic distributions. Results show that the nonoverlapped and overlapped cases are totally different in their basic characteristics. This study would contribute to further understanding unsteady electroosmotic flows in micro- and nanofluidic devices.

Key Words : Electric Double Layer (EDL), Unsteady Electroosmotic Flow, Oscillating Electric Field, Overlapped EDL

C_s, C_0	: Molar ionic concentrations
D_s, D	: Ionic diffusion coefficients
E_i, E_0	: External electric fields
e_f	: External electric-field mode
F	: Faraday constant
$H(t)$	: Heaviside function
h	: Channel half-width
k	: Parameter
M	: Grid resolution
p	: Pressure
R	: Gas constant
Sc	: Schmidt number
T	: Absolute temperature
t	: Time
U_c, U_0	: Streamwise velocities
U_{eo}	: Electroosmotic velocity
$u_i, (u,v)$	: Velocity components
$x_i, (x,y)$	: Cartesian coordinates
y'	: Normal distance from surface
z_s, z	: Ionic valences
Δt	: Transient timescale
$\Delta t_c, \Delta t_e$	: Transient timescales
$\Delta t_u, \Delta t_\omega$	: Transient timescales
δ	: Penetration depth
$\delta(y)$	: Dirac delta function
ε	: Fluid permittivity
ζ_0	: Zeta potential
ζ_0^*	: Nondimensional zeta potential
κ	: Nondimensional EDL length
λ	: EDL length
ν	: Fluid kinematic viscosity
ξ	: Parameter
ρ	: Fluid density
ρ_e	: Volumetric electric-charge density
σ_0	: Surface electric-charge density
ψ, ψ_w	: Electric potentials
ω	: External electric-field frequency
$\langle \cdot \rangle$	: Spatial averaging

* Corresponding Author,
E-mail : kangsm@dau.ac.kr
TEL : +82-51-200-7636; **FAX** : +82-51-200-7656
Department of Mechanical Engineering, Dong-A University, Busan 604-714, Korea. (Manuscript **Received** May 19, 2006; **Revised** October 13, 2006)

Subscripts

i : Indices
m : Anions
p : Cations
s : Indices (p, m)

1. Introduction

With the advent of micro- and nanofluidic devices, the electrokinetics has drawn increasingly more attention because of its feasibility and efficiency for controlling microflows in a variety of applications: for example, lab-on-a-chip, sensors and actuators, and analytical chemistry. A solid surface in contact with an infinitely large extent of electrolyte solution (e.g. ≡SiOH in aqueous solution) inherits a certain amount of charges (e.g. $\equiv SiO^-$ on the surface, either by ionization of a surface group or by ion adsorption, while the counterions are released into the solution (e.g. H^+). It leads to a formation of the electric double layer (EDL) immediately next to the surface, with a net amount of excess-counterion charges that electrically counterbalance the surface charges. Outside of the EDL, on the other hand, the bulk of the fluid is electrically neutral so that it is not affected by the surface charge. The excess counterions in the EDL move by an externally applied electric field and then drive the surrounding fluid in the EDL to move with them. Subsequently, the fluid motion in the EDL drags the fluid outside of the EDL to also move sequentially due to the fluid viscosity, finally resulting in a bulk fluid motion. Such an electrokinetic phenomenon is called the electroosmosis. Here, the characteristic thickness of the EDL, λ, often called the Debye shielding distance or EDL length, depends on the ionic concentration in the bulk of the fluid and is typically at nano scales [see Li (2004) for more details].

In this study, we assume that the electrolyte solution is composed of two species whose properties are symmetric, i.e. $z_p=-z_m=z$ where z_p and z_m are respectively the valence numbers of the cations and anions. Figure 1 shows distributions of the volumetric electric-charge density, ρ_e, for three different values of the ratio of the EDL

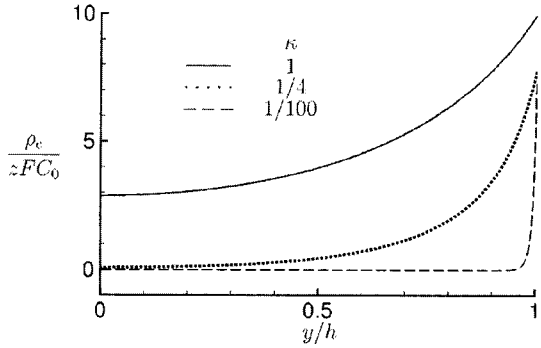

Fig. 1 Distributions of the volumetric electric-charge density in the steady state with three different nondimensional EDL lengths

length to the channel half-width (nondimensional EDL length), $\kappa=\lambda/h$, in the steady electroosmotic flow between two infinite parallel flat plates that are negatively charged. Details of the numerical method will be explained in the next section. Here, the volumetric electric-charge density is defined as

$$\rho_e=Fz(C_p-C_m) \tag{1}$$

where C_p and C_m are the molar concentrations of the cations and anions, respectively, and F the Faraday constant. Therefore, it is expected that, for the negatively charged surface, the volumetric charge density should be positive in the EDL, whereas elsewhere it should be zero so that the fluid is electrically neutral.

In case of the EDL length much smaller than the channel half-width (i.e. $\kappa=\lambda/h\ll 1$) that is typical of most microflows, the bulk of the fluid, except for the very thin EDL immediately next to the surface, has a zero volumetric charge density so that it is not affected by the external electric field (see the extreme case of $\kappa=1/100$ in Fig. 1). In that case, most of the researchers assume the Boltzmann distribution for the ionic concentrations, C_s, with little loss of accuracy, as follows:

$$C_s=C_0\exp\left(-\frac{z_sF\psi}{RT}\right) \tag{2}$$

where ψ is the electric potential due to the EDL, C_0 the molar ionic concentration in the bulk of the fluid that is electrically neutral, z_s the valence of the cations or anions, R the gas constant, and

T the absolute temperature. In a very thin EDL, the intrinsic electric-field strength ($\approx \psi_w/\lambda$ where ψ_w is the electric potential at the surface or the zeta potential) becomes very large and, if the external electric field is not extremely high, its influence on the electric field and hence on the ionic distribution is negligible in comparison with the intrinsic electric-field strength (Li, 2004). Therefore, the assumption of the Boltzmann distribution is valid in the case with the EDL length being much smaller than the channel half-width. Otherwise, however, it is no longer valid.

As the channel half-width decreases to a nanoscale comparable to the EDL length, the region of electrically neutral fluid far away from the surface becomes narrower and finally disappears (see the case of $\kappa=1/4$ in Fig. 1). With further decreasing channel half-width, the EDL's attached to the two surfaces (plates) are overlapped and thus interact with each other. In other words, the volumetric electric-charge density no longer vanishes even at the centerline (see the case of $\kappa=1$ in Fig. 1). Under the Boltzmann-distribution assumption, the ionic-concentration field should be in equilibrium and the charged surface should be in contact with an infinitely large fluid medium so that the fluid far away from the surface is electrically neutral. In such an overlapped case, therefore, the Boltzmann assumption cannot be applicable at all due to the above-mentioned second requirement even in an equilibrium state (Qu and Li, 2000 ; Li, 2004 ; Kwak and Hasselbrink, 2005). In addition, when the ionic distribution is changing with time despite the overlapped EDL's, the assumption is not valid, either.

In the present study, two kinds of unsteady flows are considered both in the nonoverlapped and overlapped EDL cases : one is the impulsive application of a constant electric field and the other is the application of a sinusoidally oscillating electric field. In the former flow, it is analyzed how the concentration fields of the cations and anions, as well as the flow field, vary with time in the transient state and finally get steady after a constant electric field is impulsively applied to an initially stagnant, electrically-neutral fluid in channel. In the latter flow, on the other hand, it is analyzed how the flow field varies with time in a fully time-periodic state when the external electric field oscillates sinusoidally.

Only a few studies have been performed on the time-evolution of the flow field for the impulsively started electroosmotic flow (Dose and Guiochon, 1993 ; Söderman and Jönsson, 1996 ; Li, 2004 ; Kwak and Hasselbrink, 2005) and for the sinusoidally oscillating electroosmotic flow (Dutta and Beskok, 2001 ; Oddy et al., 2001 ; Erickson and Li, 2003). However, most of them investigated unsteady electroosmotic flows for the very small EDL length in comparison with the channel half-width ($\kappa \ll 1$), assuming that the Boltzmann distributions were already established for the ionic concentrations before the fluid started to flow. Therefore, they had to confine themselves to the nonoverlapped EDL cases. By contrast, only an exception can be found in Kwak and Hasselbrink (2005) to our best knowledge. They performed numerical simulations on unsteady two-dimensional electroosmotic channel flow with significant EDL overlapping ($\kappa=1/3$) in the case of a constant electric field, and then found that a long nanochannel established an equilibrium state quite slowly and the timescale was determined not by diffusion across the EDL, but by diffusion or convective transport along the channel. In addition, they pursued how the concentrations of the cations and anions evolved in the transient state by solving the relevant governing equations without any assumption of the Boltzmann distribution.

The objectives of this paper are to numerically investigate unsteady two-dimensional electroosmotic flows between two infinite parallel flat plates without assuming the Boltzmann distribution, and to compare the results for the nonoverlapped EDL fields ($\kappa \ll 1$) with those for the overlapped ones ($\kappa \sim 1$). For the study, the ionic-species and electric-field equations as well as the continuity and momentum ones are solved using the finite difference method. In the present study, we assume that the external electric field is applied along the channel, that is in the streamwise direction, and the flow field is fully developed in the absence of pressure gradient. The

assumption enables one to perform numerical simulations based on the reduced one-dimensional computation (see the next section for more details). What make this study distinct from the existing ones are as follows. Firstly, this study does not assume any Boltzmann distribution for the ionic species even for the nonoverlapped EDL field, as well as for the overlapped one. Most of the existing studies assumed the Boltzmann distribution in the nonoverlapped EDL case. Especially, no investigation without any Boltzmann assumption has been performed on the oscillating electroosmotic flow to our best knowledge. Subsequently, it investigates the flow and ionic-species fields according to the ratio of the EDL length to the channel half-width for the nonoverlapped ($\kappa \ll 1$) and overlapped ($\kappa \sim 1$) EDL fields. In most of the existing studies, such an investigation has been executed separately in the nonoverlapped EDL case or in the overlapped one. Finally, it also investigates the oscillating electroosmotic flow with the overlapped EDL field. No investigation on the flow cannot be found in literature to our best knowledge. Although based on one-dimensional simulation, the present numerical method involves most difficulties that may be encountered in general multi-dimensional simulations, implying that it can be readily extended to more complex electroosmotic flows. This study would contribute to further understanding unsteady electroosmotic flows in micro- and nanofluidic devices.

2. Numerical Method

We have performed numerical simulations on unsteady two-dimensional fully-developed incompressible electroosmotic flows of a dilute two-species electrolyte solution confined between two infinite parallel flat plates apart by micro- or nano-meters. The appropriate governing equations for the flow field can be written as

$$\frac{\partial u_i}{\partial x_i}=0 \tag{3}$$

$$\frac{\partial u_i}{\partial t}+\frac{\partial u_i u_j}{\partial x}=-\frac{1}{\rho}\frac{\partial p}{\partial x_i}+\nu\frac{\partial^2 u_i}{\partial x_j \partial x_j}-\frac{\rho_e}{\rho}E_i \tag{4}$$

where x_i and u_i are respectively the Cartesian coordinates and their corresponding velocity components, t the time, E_i the external electric-field components, p the pressure, ρ the fluid density, and v the kinematic viscosity. Here, the electroosmotic flow can be driven through the body force term, $-\rho_e E_i/\rho$, in Eq. (4), that is through interaction between the electric-charge distribution in the fluid and the external electric field.

As already mentioned, we assume that, with the absence of pressure gradient, the flow field is fully developed in the streamwise direction. In such a case, since the convection term can be neglected in Eq. (4), the two-dimensional fully-developed electroosmotic channel flow reduces to one-dimensional problem (Dutta and Beskok, 2001; Oddy et al., 2001; Li, 2004). With the fully-developed assumption, the governing equation for the streamwise velocity, u, can be rewritten as

$$\frac{\partial u}{\partial t}=\nu\frac{\partial^2 u}{\partial y}-\frac{\rho_e}{\rho}E_0 e_f \tag{5}$$

where y is the surface-normal coordinate with its origin at the centerline ($y=0$) and E_0 the external electric field applied along the channel. The external electric-field forcing mode, e_f, is given as follows:

$$e_f=\begin{cases}H(t)\\ \sin(2\pi\omega t)\end{cases} \tag{6}$$

where $H(t)$ is the Heaviside function [$H(t)=1$ for $t\geq 0$ and otherwise $H(t)=0$] and the external electric-field forcing frequency. Notice that, in Eq. (6), the former electric-field forcing mode corresponds to the impulsively started electroosmotic flow while the latter mode does to the sinusoidally oscillating one.

With the fully-developed assumption, the molar concentrations of the cations and anions, C_p and C_m, can be obtained from the following species equations (Hu et al., 1999; Lin et al., 2004; Kwak and Hasselbrink, 2005; Qian and Bau, 2005):

$$\frac{1}{D}\frac{\partial C_p}{\partial t}=\frac{\partial^2 C_p}{\partial y^2}+\frac{zF}{RT}\frac{\partial}{\partial y}\left[C_p\frac{\partial \psi}{\partial y}\right] \tag{7}$$

$$\frac{1}{D}\frac{\partial C_m}{\partial t}=\frac{\partial^2 C_m}{\partial y^2}-\frac{zF}{RT}\frac{\partial}{\partial y}\left[C_m\frac{\partial \psi}{\partial y}\right] \tag{8}$$

where D is the ionic diffusion coefficient (we have already assumed that the electrolyte solution is symmetric, i.e. $D_p=D_m=D$ and $z_p=-z_m=z$). The electric potential due to the EDL, ψ, satisfies the following one-dimensional Poisson equation (Li, 2004):

$$\varepsilon\frac{\partial^2\psi}{\partial y^2}=-\rho_e \tag{9}$$

where ε is the fluid permittivity. Notice that, since ρ_e is not constant, the above equation cannot be readily integrated. Equations (5) and (7)-(9) constitute a set of governing differential equations for predicting unsteady electroosmotic flows and ionic distributions in the nonoverlapped and overlapped cases. Notice also that the governing equations are free from the Boltzmann-distribution assumption.

Most materials obtain electric charges when they are brought into contact with an aqueous solution and various plausible explanations for such an phenomenon can be found in literature (Li, 2004). In the present study, we assume that a certain amount of cations are released from the surface into the fluid due to ionization of a surface group, resulting in a negatively charged surface. That is, the net amounts of electric charges on the surface and in the fluid are equal in strength but different in sign, leading to the following relation (in case of the two-dimensional fully-developed electroosmotic channel flow) (Li, 2004; Kwak and Hasselbrink, 2005):

$$2\sigma_0=-\int_{-h}^{h}\rho_e dy \tag{10}$$

where σ_0 is the surface electric-charge density and h the channel half-width. Notice that the EDL zeta potential, ζ_0, can be estimated, using a simple dimensional analysis, as

$$\zeta_0=\frac{\sigma_0\lambda}{\varepsilon} \tag{11}$$

To solve the second-order differential equations (5) and (7)-(9), appropriate boundary conditions are necessary at the two surfaces ($y=\pm h$). Numerical simulations are performed only on the upper half-channel ($0\le y\le h$) due to the geometric and physical symmetry and, thus, no-gradient rule, $\partial/\partial y$, is applied for the dependent variables (u, C_p, C_m and ψ) at the centerline ($y=0$). On the other hand, the boundary conditions at the upper surface ($y=h$) are given as:

$$u=0 \tag{12}$$

$$\frac{\partial C_p}{\partial y}=-\frac{zF}{RT}\frac{\sigma_0}{\varepsilon}C_p \tag{13}$$

$$\frac{\partial C_m}{\partial y}=\frac{zF}{RT}\frac{\sigma_0}{\varepsilon}C_m \tag{14}$$

$$\frac{\partial\psi}{\partial y}=\frac{\sigma_0}{\varepsilon} \tag{15}$$

The first one corresponds to the no-slip condition, the next two ones to the no-flux of the cations and anions through the solid surface, and the last one to the condition of a constant surface electric-charge density.

The governing differential equations, (5) and (7)-(9), are integrated in time using a second-order semi-implicit fractional-step method: a third-order Runge-Kutta method (RK3) for the electric body-force term and a second-order Crank-Nicolson method for the diffusion terms. In space, on the other hand, the governing equations are resolved with a finite-difference approach and all the spatial derivatives are discretized with the second-order central difference scheme. The non-uniform spatial grids are generated using the tangential hyperbolic function with a resolution of $M=257$ such that the near-wall region is more resolved. To validate the code, a numerical simulation has been performed on the impulsively started electroosmotic flow for $\kappa=1/3$ and its results are compared with Kwak and Hasselbrink (2005). Details of the comparison will be explained in the next section. The section also contains the numerical results for the impulsively started electroosmotic flow and sinusoidally oscillating one.

3. Results

In the present study, numerical simulations have been performed mainly for $\kappa=\lambda/h=1/100$ and 1 to predict unsteady electroosmotic flows re-

spectively in the nonoverlapped and overlapped EDL cases, where λ is the EDL length defined as (Li, 2004)

$$\lambda=\left[\frac{\varepsilon RT}{2F^2z^2C_0}\right]^{1/2} \tag{16}$$

For the study, we consider a symmetric unary electrolyte, that is $z_p=-z_m=z=1$. In addition, the nondimensional zeta potential is set to be $\zeta_0^*\equiv Fz\zeta_0/RT=-2.35$ (corresponding to $\zeta_0=$ 60 mV at 20℃) and the Schmidt number is $Sc=\nu/D$, following the study of Kwak and Hasselbrink (2005).

3.1 Impulsively started electroosmotic flow

At first, we have numerically investigated how the fluid flow and ionic distributions vary with time in the transient state for the impulsively started electroosmotic flow in the nonoverlapped and overlapped EDL cases. For the study, numerical simulations start immediately after the impulsive application of a constant external electric field [$e_f=H(t)$], in concurrence with the impulsive contact of the surface with a stagnant, electrically-neutral aqueous solution. Notice that, immediately after the impulsive contact, a certain amount of cations are released into the fluid and simultaneously the surface becomes negatively charged [refer to Eq. (10)]. It is assumed, subsequently, that the cations released from the surface are accumulated in the the extremely thin layer immediately next to the surface [see Kwak and Hasselbrink (2005) for more details]. On the other hand, the electric field due to the EDL, ψ, at the initial instant can be obtained by directly solving the Poisson equation (9).

To validate the code, a numerical simulation has been performed on unsteady electroosmotic flow for $\kappa=\lambda/h=1/3$ and the typical results are compared with those obtained from the two-dimensional simulation by Kwak and Hasselbrink (2005). Figure 2 shows distributions of the anion concentration and streamwise velocity at two different times, $tD/h^2=0.03$ and 1.0, in case of $\kappa=1/3$, compared with those of Kwak and Hasselbrink (2005). Exact agreement between our results and Kwak and Hasselbrink's ones is found in the figure, implying that the present numerical method can well predict the unsteady electroosmotic flows and ionic distributions. In the figure, U_{eo} is the electroosmotic velocity, defined as

$$U_{eo}\equiv\frac{\varepsilon\zeta_0E_0}{\rho\nu}=\frac{\sigma_0\lambda E_0}{\rho\nu} \tag{17}$$

Equation (17) is well known as the Helmholtz-Smoluchowski formulation which relates the electroosmotic velocity, U_{eo}, to the surface zeta potential, ζ_0, and external electric field, E_0.

After verifying the numerical method, we have conducted numerical simulations for $\kappa=1/100$ (nonoverlapped case) and (overlapped case), whose results are shown in Figs. 3 and 4, respectively.

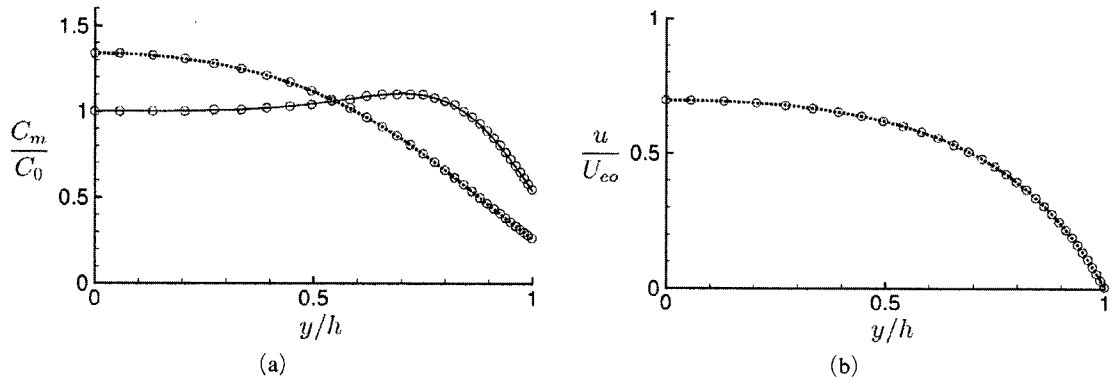

Fig. 2 Validation of the numerical method : distributions of (a) the anion concentration and (b) streamwise velocity at different times, $tD/h^2=0.03$ (solid lines) and 1.0 (dotted lines), in the transient state for $\kappa=\lambda/h=1/3$, compared with those (denoted by ○) obtained from the two-dimensional simulation by Kwak and Hasselbrink (2005)

Figure 3 shows the time-evolution of the streamwise velocity and ionic concentrations in the transient state for the nonoverlapped EDL case. Notice that, since the flow is fully developed and thus the convection terms in Eqs. (7) and (8) automatically vanish, the ionic concentrations are decoupled from the streamwise velocity. At first, to see if the electroosmotic flow becomes steady, the time traces of the streamwise velocity at the centerline ($y/h=0$) and the anion concentration at the surface ($y/h=1$) are shown in Fig. 3(a). The traces indicate that the fluid flow and ionic distributions vary with time in the early stage and then finally become steady. Subsequently, the distributions of the streamwise velocity and cation and anion concentrations at different times in the transient state, together with the steady solutions, are shown in Figs. 3(b)-(d), respectively.

As expected, the flow and ionic-concentration fields change sharply across the EDL immediately next to the surface that is very thin in comparison with the channel half-width. The cations released from the surface immediately after the impulsive contact of the fluid and solid surface are transported toward the centerline due to the ionic diffusion and then finally attain a new equilibrium state (steady state), while the cations are assembled at high concentration in the very thin EDL due to the attractive force with the negatively charged surface [see Fig. 3(c)]. On the other hand, the anions that are uniformly distributed at the initial instant ($C_m=C_0$) move toward the centerline due to the repulsive force from the surface [see Fig. 3(d)]. While the anions move, they have a convex-shaped distribution owing to their conservation law and their concentration at the surface steeply decreases. Notice that, the fluid has excess cations in the very thin EDL, whereas in the bulk of the fluid it is electrically neutral (see also Fig. 1). Here, it is notable to

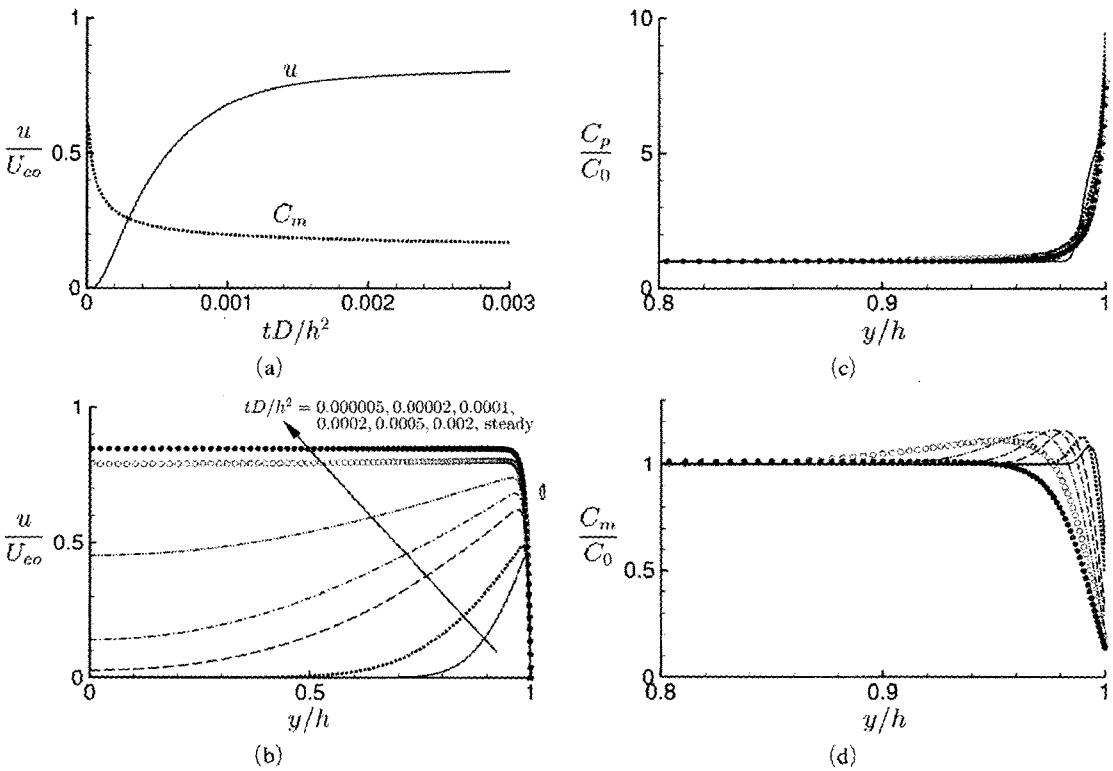

Fig. 3 (a) Time-evolution of the streamwise velocity at $y/h=0$ and the anion concentration at $y/h=1$, and profiles of (b) the streamwise velocity and (c), (d) cation and anion concentrations in the transient state under a constant electric field [$e_f=H(t)$] for $\kappa=\lambda/h=1/100$ in the overlapped case

mention why the average of volumetric electric-charge density varies with the nondimensional EDL length in Fig. 1. In this study, we assume that the surface electric-charge density, σ_0, is constant. From Eq. (10), we can derive $\langle \rho_e \rangle = -\sigma_0/h$, or $\langle \rho_e \rangle / zFC_0 = 2\kappa\zeta_0^*$, where $\langle \cdot \rangle$ is the y-spatial average, implying that the volumetric electric-charge density augments linearly with increasing nondimensional EDL length for a constant ζ_0^* in this study.

The time-evolution of the streamwise-velocity distribution is shown in Fig. 3(b). Excess cations being formed in the very thin EDL move due to their interaction with the external electric field and then drive the surrounding fluid in the EDL to move with them. Subsequently, the fluid motion in the EDL drags the fluid outside of the EDL to also move sequentially due to the fluid viscosity, finally resulting in a plug-type velocity profile across the channel. That is, after a sufficiently long time, i.e. in the steady state, the flow becomes flat in its velocity distribution. It is mainly due to no significant physical force involved in the bulk of the fluid outside of the EDL and a finite streamwise velocity at the edge of the EDL. In the very early stage, i.e. $tD/h^2 \lesssim 0.0001$, it is found that the effect of the finite streamwise velocity at the edge keeps on penetrating into the bulk of the stagnant fluid and, thus, the stagnant fluid still remains in the central region, as obviously shown in Fig. 3(b). Such a phenomenon is very similar to the Stokes' first problem where the infinitely large extent of stagnant fluid also moves due to the impulsively started surface motion (Currie, 1974). However, since the ionic-concentration fields in the EDL and, thus, the streamwise velocity at the edge of the EDL still change even in the transient state, the present electroosmotic flow is somewhat different from Stokes' first problem.

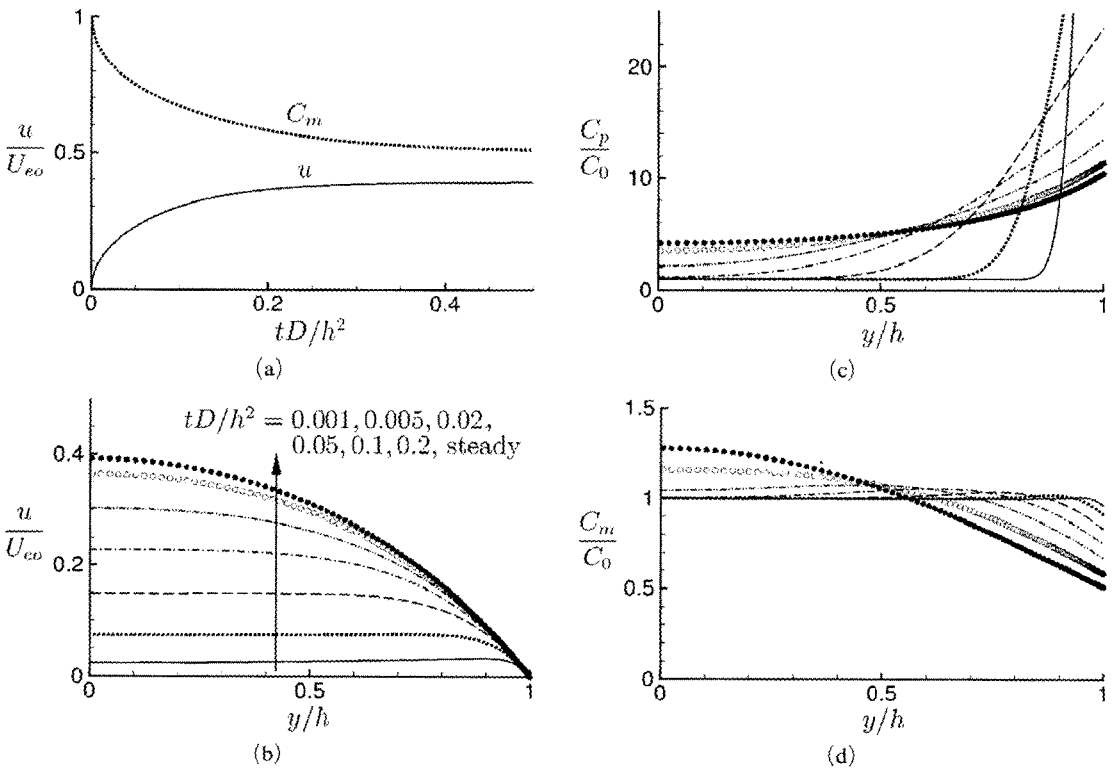

Fig. 4 (a) Time-evolution of the streamwise velocity at $y/h=0$ and the anion concentration at $y/h=1$, and profiles of (b) the streamwise velocity and (c), (d) cation and anion concentrations in the transient state under a constant electric field $[e_f=H(t)]$ for $\kappa=\lambda/h=1$ in the overlapped case

It is remarkable to estimate the transient timescales for reaching a steady (or quasi-steady) state in the nonoverlapped case where the EDL is negligibly thin in comparison with the channel half-width ($\kappa \ll 1$), i.e. $\kappa = 1/100$. A simple dimensional analysis on Eqs. (5) and (7)-(8) provides with the following three transient timescales:

$$\frac{\Delta t_u D}{h^2} \sim \frac{1}{\mathrm{Sc}}, \quad \frac{\Delta t_c D}{h^2} \sim \kappa^2, \quad \frac{\Delta t_e D}{h^2} \sim \frac{\kappa^2}{(-\zeta_0^*)} \tag{18}$$

Here, the first timescale comes from the viscous effect of fluid, while the second and third ones come from the diffusion and electric-field effects of ions, respectively. Notice that, since $\Delta t_c > \Delta t_e$ for any κ (we assumed that $\zeta_0^* = -2.35$ in this study), the transient timescale can be estimated by the bigger one out of Δt_u and Δt_c. In case of $\kappa = 1/100$ and $\mathrm{Sc} = 1000$, $\Delta t_u \sim 0.001 h^2/D$ and $\Delta t_c \sim 0.0001 h^2/D$, implying that the fluid-viscosity effect is dominant in determining the transient timescale: $\Delta t \sim 0.001 h^2/D$ (for example, $\Delta t \sim 1\ \mu s$ for $h = 1\ \mu m$ and $D = 10^{-9} m^2/s$). Such an estimation is in fairly good agreement with the result indicated in Fig. 3(a).

Figure 4, on the other hand, shows the corresponding simulation results in the overlapped EDL case, i.e. $\kappa = 1$. Results indicate that the characteristics in the overlapped case are basically different from those in the nonoverlapped case. It is found that, in the overlapped case, since the EDL length is comparable to the channel half-width, that is $\lambda \sim h$ (even if $\lambda = h$ in the present case), all the variables, such as the ionic concentrations and thus the streamwise velocity, change all over the channel. In other words, there exists no electrically neutral region in the channel (see also Fig. 1), indicating that the assumption of the Boltzmann distribution is not valid at all in the overlapped case.

As indicated in Figs. 4(c) and (d), the cations that are released from the surface at the initial instant are transported toward the centerline mainly through the ionic diffusion due to their very high concentration near the surface (the cations must also move toward the surface due to the attractive force with the negatively charged surface, but its effect is relatively small in comparison with the diffusion effect). That is, the cation concentration at the centerline increases with time in the transient state, while at the surface it decreases. On the other hand, the anions move toward the centerline, mainly due to the repulsive force from the negatively charged surface. In the long run, the ionic distributions reach a steady state. Since the fluid has a positive volumetric electric-charge density, that is excess cations, all over the channel, the external electric field drives all the fluid in channel to move nearly at the same time from the initial instant, leading to a flat velocity distribution in the early stage. As the time goes by, the flow rate through the channel increases, but more rapidly near the centerline than near the surface due to the viscous effect of surface, resulting in a parabolic velocity distribution at the steady state. Such an observation can be obviously found from Fig. 4(b).

Comparison between Figs. 3(a) and 4(a) indicates that it takes longer for the flow to reach a steady state in the overlapped case than in the nonoverlapped case for the same channel half-width. The relations, $\Delta t_u \sim 0.001 h^2/D$ and $\Delta t_c \sim h^2/D$ (owing to $\kappa \sim 1$) in Eq. (18), imply that the transient timescale can be determined mainly by the ionic diffusion effect: $\Delta t \sim h^2/D$ (for example, $\Delta t \sim 1$ ms for $h = 1\ \mu m$ and $D = 10^{-9} m^2/s$). This estimation is in approximately good agreement with that in Fig. 4(a). Collectively speaking, the transient timescale in the overlapped case is determined mainly by the ionic diffusion, whereas in the nonoverlapped case it is mainly by the fluid viscosity. Therefore, the former timescale is much longer than the latter one (h^2 versus $0.001 h^2/D$).

3.2 Sinusoidally oscillating electroosmotic flow

Subsequently, we have investigated how the fluid flow varies with time in the fully time-periodic state for the sinusoidally oscillating electroosmotic flow in the nonoverlapped and overlapped EDL cases. For the study, numerical simulations are performed by externally applying a sinusoidally oscillating electric field along the channel [$E_0 e_x = E_0 \sin(2\pi\omega t)$]. Notice that, since

the ionic-species equations (7)-(8) are decoupled from the streamwise momentum equation (5), the change in the forcing mode, i.e. from $e_f=H(t)$ to $e_f=\sin(2\pi\omega t)$, exerts no effect on the ionic distributions (C_p and C_m) and thus the electric field (ψ), but does an effect on the streamwise velocity (u). In the fully time-periodic state, therefore, only the streamwise velocity becomes fully time-periodic, whereas the ionic distributions and thus the electric field keep the steady state in the same way as in the constant external electric-field case (see Fig. 1). Figures 5 and 6 show the time-evolution of the sinusoidally oscillating electroosmotic flow in the fully time-periodic state for the nonoverlapped and overlapped EDL cases, respectively.

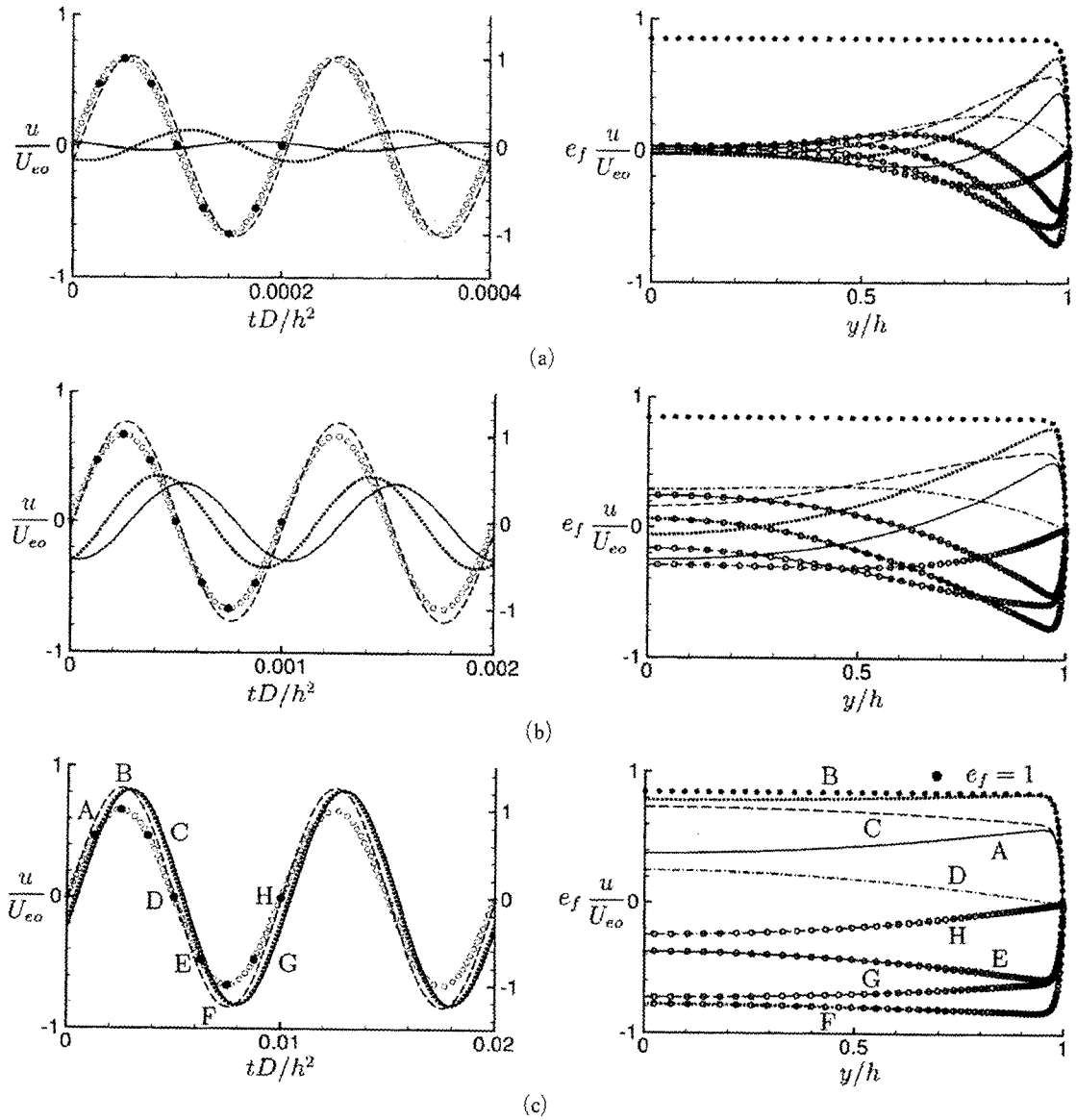

Fig. 5 (a) Time-evolution of the streamwise velocities at $y/h=0$ (solid lines), 0.5 (dotted lines) and 0.95 (dashed lines) together with the forcing mode (e_f) (denoted by ○) (left side), and profiles of the streamwise velocity (right side), in the fully time-periodic state under an oscillating electric field [$e_f=\sin(2\pi\omega t)$] for $\kappa=\lambda/h=1/100$ in the overlapped case: $\omega h^2/D=$ (a) 5000, (b) 1000 and (c) 100

The plots on the left hand side in Fig. 5 show the time-evolution of the streamwise velocities at $y/h=0$ (at the centerline), 0.5 and 0.95 (near the surface), together with $e_f=\sin(2\pi\omega t)$, at different forcing frequencies, $\omega h^2/D=5000$, 1000 and 100, for $\kappa=1/100$ in the nonoverlapped case (for example, $\omega=5$ MHz, 1 MHz and 100 kHz for $h=1$ μm and $D=10^{-9}$m^2/s, respectively). Results indicate that in all cases the flow oscillates in the streamwise direction at the same frequency as the external electric field. Here, since the oscillating electric field affects only the very thin EDL immediately next to the surface, the corresponding oscillating flow occurs near the surface, i.e. at $y/h=0.95$, and its streamwise velocity has nearly the same phase with the electric-field forcing mode.

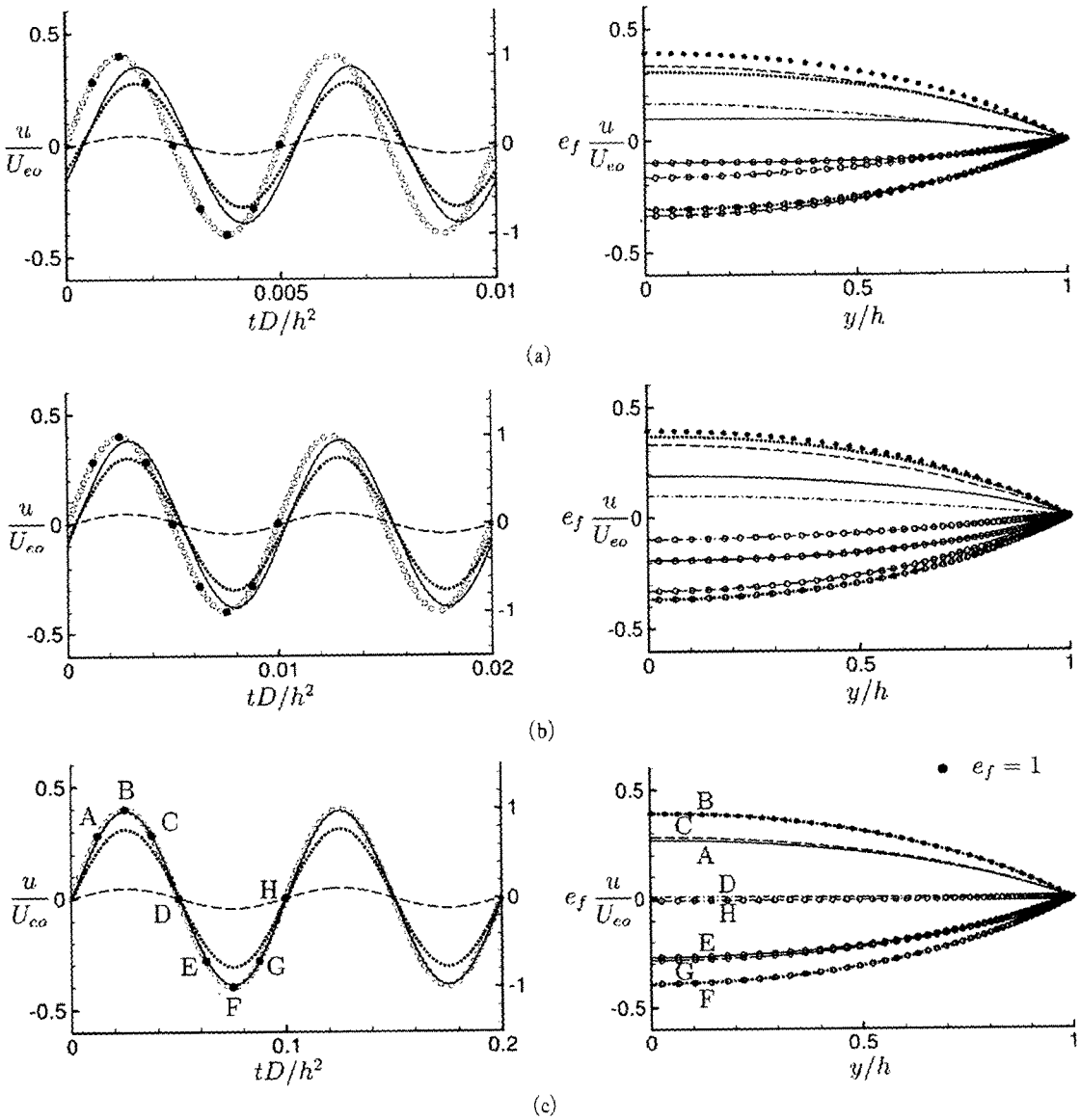

Fig. 6 (a) Time-evolution of the streamwise velocities at $y/h=0$ (solid lines), 0.5 (dotted lines) and 0.95 (dashed lines) together with the forcing mode (e_f) (denoted by ○) (left side), and profiles of the streamwise velocity (right side), in the fully time-periodic state under an oscillating electric field [$e_f=\sin(2\pi\omega t)$] for $\kappa=\lambda/h=1$ in the overlapped case: $\omega h^2/D=$ (a) 200, (b) 100 and (c) 10

Subsequently, the effect of oscillating flow in the EDL propagates sequentially into the stagnant fluid outside of the EDL due to the fluid viscosity, leading to an oscillating bulk flow in channel. Therefore, the oscillating flow away from the edge of the EDL lags behind the external electric field, and the phase lag augments with increasing distance from the edge. Such a phenomenon can be obviously found on the left hand side in Fig. 5.

It is remarkable to mention that the sinusoidally oscillating electroosmotic flow at a very high frequency, i.e. $\omega h^2/D=5000$ [see Fig. 5(a)], is very similar to the Stokes' second problem where an infinitely large extent of stagnant fluid also oscillates due to the sinusoidally oscillating surface motion (Currie, 1974). The streamwise velocity in the Stokes' second problem is given, in an analytical form, as

$$u(y',t)=U_0\exp(-ky')\sin(2\pi\omega t-ky') \quad (19)$$

where U_0 denotes the amplitude in the surface velocity, y' the normal distance from the surface, and $k=\sqrt{\pi\omega/\nu}$. Figure 7 shows comparison of the velocity profiles between the sinusoidally oscillating electroosmotic flow and the Stokes' second problem at the same frequency, $\omega h^2/D=5000$. Here, the surface velocity, U_0, is set equal to the velocity at the centerline obtained in the steady state for the constant electric-field case [see Fig. 3(b)]. It is seen that the two velocity profiles are in exact agreement with each other except for the near-surface region, indicating the analogy of the unsteady electroosmotic flow to the Stokes' second problem. Such analogy can also be found in Dutta and Beskok (2001).

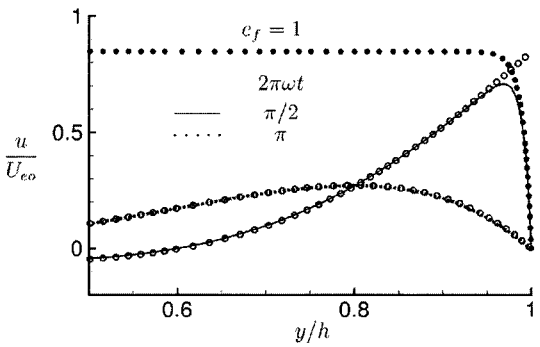

Fig. 7 Profiles of the streamwise velocity at $2\pi\omega t=\pi/2$ and π in the fully time-periodic state for $\omega h^2/D=5000$ together with the constant electric-field case, compared to the Stokes' second problem (denoted by ○)

To investigate its meaning, the parameter k appearing in Eq. (19) can be rewritten, in the nondimensional form, as

$$(kh)^2=\pi\frac{1/\mathrm{Sc}}{D/\omega h^2}=\pi\frac{(1/\mathrm{Sc})\,(h^2/D)}{1/\omega}\sim\frac{\Delta t_u}{\Delta t_\omega} \quad (20)$$

where Δt_u and Δt_ω are respectively the transient timescales due to the fluid viscosity and due to the oscillation. Therefore, the nondimensional parameter $(kh)^2$ can be estimated as the ratio of the viscous transient timescale to the oscillation one. With decreasing electric-field forcing frequency, the oscillation timescale increases and thus the nondimensional parameter, $(kh)^2$, decreases. In such a case, the oscillation effect in the very thin EDL penetrates deeper into the stagnant bulk fluid. In other words, the penetration depth, sometimes defined as $\delta=2/k$ (Curie, 1974), increases with decreasing forcing frequency and consequently it becomes larger than the channel half-width ($\delta>h$) at a forcing frequency lower than a certain critical value. It implies that the oscillating flow developed by one EDL interacts with that by the other EDL and, thus, its analogy with the Stokes' second problem is not valid any longer. At such a low forcing frequency, nevertheless, the characteristics of amplitude and phase lag in the streamwise velocity can be approximately understood using the analogy with the Stokes' second problem. On the other hand, the plots on the right hand side in Fig. 5 show profiles of the corresponding streamwise velocity at 8 equi-spaced different times in one complete period, together with the constant electric-field case for comparison.

As can be already estimated from Eq. (19), the amplitude of the streamwise velocity that has its maximum value in the very thin EDL decays exponentially with increasing distance from the edge

of the EDL. At the same time, the decaying rate diminishes with decreasing forcing frequency and thus $k=\sqrt{\pi\omega/\nu}$. Dutta and Beskok (2001) investigated analytically the sinusoidally oscillating electroosmotic flow by assuming the Boltzmann distribution, and found that, depending on $\xi=\sqrt{2}\kappa kh\sim\sqrt{\omega}$ for a constant $\kappa=1/100$ in this study, the flow ranges from a case analogous to the Stokes' second problem (for high ξ) to an oscillatory "pluglike" flow (for low ξ). Their finding is in excellent agreement with the present observation: the former flow corresponds to $\omega h^2/D=5000$ in Fig. 5(a) while the latter one does to $\omega h^2/D=100$ in Fig. 5(c). Equation (19) also shows that there is a phase lag in the bulk flow and the phase lag varies proportionally to the distance from the edge. In addition, the variation rate diminishes with decreasing forcing frequency and thus $k=\sqrt{\pi\omega/\nu}$. In other words, it can be clearly observed from the left-side plots in Fig. 5 that the phase lag diminishes with decreasing forcing frequency and disappears at $\omega h^2/D\lesssim 100$.

Figure 6 shows the time-evolution of the streamwise-velocity profile in the fully time-periodic state under an external electrical field oscillating at $\omega h^2/D=200$, 100 and 10 for $\kappa=1$ in the overlapped EDL case (for example, $\omega=200$ kHz, 100 kHz and 10 kHz for $h=1$ μm and $D=10^{-9}$ m^2/s, respectively). The figure indicates that the flow characteristics in the overlapped case are basically different from those in the nonoverlapped case. As evidently shown in Figs. 3(a) and 4(a), the transient timescale for the overlapped case is much larger than that for the nonoverlapped case. Consequently, the unsteady effect due to the oscillating electric field can occur at the forcing frequency much lower than the nonoverlapped case.

Since the volumetric electric-charge density is positive all over the channel due to the large nondimensional EDL length ($\lambda\sim h$) (see Fig. 1), all the fluid in channel is concurrently driven to also oscillate by the oscillating external electric field. Unlike the nonoverlapped case, therefore, the amplitude in the streamwise velocity is very small near the surface because of the viscous effect from the surface, and then increases gently with the distance from the surface, leading to a parabolic distribution in the amplitude. At a relatively high forcing frequency, i.e. $\omega h^2/D=200$, there is a comparatively large phase lag between the electric-field forcing mode and the flow motion near the surface, i.e. at $y/h=0.95$, but little phase lag through the fluid inside the channel [see Fig. 6(a)]. Such an observation is much different from the nonoverlapped case. In the nonoverlapped case, the phase lag that is very small near the surface increases linearly with the distance from the surface (or the edge of the EDL). In the overlapped case, on the other hand, the phase lag that is comparatively large near the surface hardly vary with the distance. The phase lag between the forcing mode and fluid flow diminishes with decreasing forcing frequency and finally approaches zero when the frequency exceeds a certain critical value, i.e. $\omega h^2/D=10$ [see Fig. 6(c)]. At such a low forcing frequency, the amplitude distribution of the streamwise velocity also becomes equal to that obtained for the constant electric field.

4. Conclusions

In this paper, we have numerically investigated unsteady two-dimensional fully-developed electroosmotic flows between two infinite parallel flat plates in the nonoverlapped and overlapped EDL cases without any assumption of the Boltzmann distribution. Notice that the Boltzmann assumption is valid only when the EDL's are not overlapped and the ionic distributions establish equilibrium. For the study, two kinds of unsteady flows were considered: one was the impulsive application of a constant electric field [$e_f=H(t)$] and the other was the application of a sinusoidally oscillating electric field [$e_f=\sin(2\pi\omega t)$]. Two nondimensional EDL lengths, $\kappa=\lambda/h=1/100$ and 1 where λ denotes the EDL length and h the channel half-width, were selected respectively for the nonoverlapped and overlapped cases. For the numerical simulations, the ionic-species and electric-field equations as well as the continuity and momentum ones were solved using the finite

difference method. Here, it was assumed that a constant surface electric-charge density was imposed on the two surfaces.

At first, we performed numerical simulations on the impulsively started electroosmotic flow, and then found that the ionic distributions and thus the flow field varied with time in the early stage, leading to a steady state in the long run. In addition, the nonoverlapped and overlapped cases were totally different in their basic characteristics. In the nonoverlapped case, the transient timescale was determined mainly by the fluid viscosity and the flow in the steady state was characterized by a flat velocity distribution. In the overlapped case, on the other hand, the timescale that was determined mainly by the ionic diffusion was much smaller than that in the nonoverlapped case. Besides, the flow became of a parabolic velocity distribution after a sufficiently long time.

Subsequently, we performed numerical simulations on the sinusoidally oscillating electroosmotic flow, and then found that the flow oscillated in the streamwise direction at the same frequency as the external electric field. In addition, the flow characteristics in the nonoverlapped and overlapped cases were basically different. In the nonoverlapped case, the flow at a very high frequency was very similar to the Stokes' second problem : the amplitude in the streamwise velocity that had its maximum value in the very thin EDL decayed exponentially with the distance from the edge of the EDL and the phase lag with respect to the electric-field forcing mode increased linearly. With decreasing forcing frequency, the amplitude became flatter in its distribution while the phase lag diminished. In the overlapped case, on the other hand, the unsteady effect due to the oscillation could be attained at the forcing frequency much lower than the nonoverlapped case. The amplitude was parabolic in its distribution regardless of the forcing frequency. For a relatively high forcing frequency, there was a comparatively large phase lag between the forcing mode and the flow near the surface, but little phase lag through the fluid in channel. The phase lag near the surface diminished with decreasing forcing frequency.

Acknowledgments

This work was supported by the NRL (National Research Laboratory) Program of the Ministry of Science and Technology, Korea.

References

Currie, I. G., 1974, *Fundamental Mechanics of Fluids*, McGraw-Hill, New York.

Dose, E. V. and Guiochon, G., 1993, "Timescales of Transient Processes in Capillary Electrophoresis," *Journal of Chromatography A*, Vol. 652, pp. 263~275.

Dutta, P. and Beskok, A., 2001, "Analytical Solution of Time Periodic Electroosmotic Flows : Analogies to Stokes' Second Problem," *Analytical Chemistry*, Vol. 73, pp. 5097~5102.

Erickson, D. and Li, D., 2003, "Analysis of Alternating Current Electroosmotic Flows in a Rectangular Microchannel," *Langmuir*, Vol. 19, pp. 5421~5430.

Hu, L., Harrison, J. D., and Masliyah, J. H., 1999, "Numerical Model of Electrokinetic Flow for Capillary Electrophoresis," *Journal of Colloid and Interface Science*, Vol. 215, pp. 300~312.

Kwak, H. S. and Hasselbrink Jr., E. F., 2005, "Timescales for Relaxation to Boltzmann Equilibrium in Nanopores," *Journal of Colloid and Interface Science*, Vol. 284, pp. 753~758.

Li, D., 2004, *Electrokinetics in Microfluidics*, Elsevier, London.

Lin, H., Storey, B. D., Oddy, M. H., Chen, C. -H. and Santiago, J. G., 2004, "Instability of Electrokinetic Microchannel Flows with Conductivity Gradients," *Physics of Fluids*, Vol. 16, pp. 1922~1935.

Oddy, M. H., Santiago, J. G. and Mikkelsen, J. C., 2001, "Electrokinetic Instability Micromixing," *Analytical Chemistry*, Vol. 73, pp. 5822~5832.

Qian, S. and Bau, H. H., 2005, "Theoretical Investigation of Electro-osmotic Flows and Chaotic Stirring in Rectangular Cavities," *Applied Mathematical Modelling*, Vol. 29, pp. 726~753.

Qu, W. and Li, D., 2000, "A Model for Over-

lapped EDL Fields," *Journal of Colloid and Interface Science*, Vol. 224, pp. 397~407.

Söderman, O. and Jönsson, B., 1996, "Electro-osmosis: Velocity Profiles in Different Geometries with Both Temporal and Spatial Resolution," *Journal of Chemical Physics*, Vol. 105, pp. 10300~10311.

Stone, H. A., Stroock, A. D. and Ajdari, A., 2004, "Engineering Flows in Small Devices: Microfluidics toward a Lab-on-a-Chip," *Annual Review of Fluid Mechanics*, Vol. 36, pp. 381~411.